Annu. Rev. Biophys. Biomol. Struct. 2002. 31:257–73
DOI: 10.1146/annurev.biophys.31.082901.134439

THE SEARCH AND ITS OUTCOME: High-Resolution Structures of Ribosomal Particles from Mesophilic, Thermophilic, and Halophilic Bacteria at Various Functional States

Ada Yonath
Department of Structural Biology, Weizmann Institute of Science, Rehovot 76100, Israel and Max-Planck-Research Unit for Ribosomal Structure, Hamburg 22603, Germany; e-mail: ada.yonath@weizmann.ac.il

Key Words ribosomes, large ribosomal subunit, small ribosomal subunit, flexibility, initiation, antibiotics

■ **Abstract** We determined the high-resolution structures of large and small ribosomal subunits from mesophilic and thermophilic bacteria and compared them with those of the thermophilic ribosome and the halophilic large subunit. We confirmed that the elements involved in intersubunit contacts and in substrate binding are inherently flexible and that a common ribosomal strategy is to utilize this conformational variability for optimizing its functional efficiency and minimizing nonproductive interactions. Under close-to-physiological conditions, these elements maintain well-ordered characteristic conformations. In unbound subunits, the features creating intersubunit bridges within associated ribosomes lie on the interface surface, and the features that bind factors and substrates reach toward the binding site only when conditions are ripe.

CONTENTS

INTRODUCTION

Ribosomes are the universal cellular organelles that catalyze the sequential polymerization of amino acids according to the genetic blueprint encoded in the mRNA. They are built of two subunits that associate for performing this task. The larger subunit creates the peptide bonds and provides the path for the progression of the nascent proteins. The smaller subunit has key roles in the initiation of the process, in decoding the genetic message, in discriminating against non- and near-cognate aminoacylated tRNA molecules, in controlling the fidelity of codon-anti-codon interactions, and in mRNA/tRNA translocation. The prokaryotic large ribosomal subunit (50S) has a molecular weight of 1.5×10^6 Dalton and contains two RNA chains with a total of ~3000 nucleotides and ~35 proteins. The small ribosomal subunit (called 30S) has a molecular weight of 8.5×10^5 Dalton and contains one RNA chain of over 1500 nucleotides and ~20 proteins.

Over two decades ago, we initialized a long and demanding search for the determination of the three-dimensional structure of the ribosome by X-ray crystallography (74). The key to high-resolution data was to crystallize homogenous preparations under conditions similar to their in situ environments or to induce a selected conformation after the crystals were formed. Relatively robust ribosomal particles were chosen, assuming that they would deteriorate less during preparation and therefore provide more homogenous starting materials for crystallization.

The first crystals to yield some crystallographic information (e.g., symmetry, unit cell parameters, and resolution) were of the large subunit from *Bacillus stearothermophilus* (71) and *Haloarcula marismortui* (H50S) (39, 66). Shortly afterward, we characterized crystals of the small subunit from *Thermus thermophilus* (T30S) (72). Microcrystals of the same source were grown independently at approximately the same time (64).

An alternative approach was to design complexes containing ribosomes at defined functional stages, such as of the entire ribosome with two tRNA molecules and a short mRNA analog (27). This approach was later adopted, refined, and extended and has led a medium-resolution structure of the ribosome with three tRNA molecules (75). It is interesting that, until recently, the only crystals that led to high-resolution structures worldwide were of these two sources, H50S (4) and T30S (53, 69). As discussed below and in (5, 28), this situation has now changed since we identified a robust ribosome from a mesophilic eubacterium that crystallizes well under mild conditions in the presence and in the absence of antibiotics and substrate analogs.

All ribosomal crystals presented challenging technical problems, resulting from their enormous size, complexity, natural tendency to deteriorate and disintegrate, internal flexibility, and their sensitivity to irradiation. For minimizing the harm caused by the latter, we pioneered crystallographic data collection at cryogenic temperatures (32). This, together with the dramatic advances of the X-ray sources, namely the third-generation synchrotrons equipped with state-of-the-art detectors and increased sophistication in phasing, enabled us, as well as others, to handle

most of the technical problems. Consequently, structures of ribosomal particles are currently emerging at an impressive speed (4, 28, 53, 69). This chapter focuses on the functional relevance of one of the characteristic properties of ribosomal particles: their inherent conformational variability.

From the initial stage of our studies, we aimed at the elucidation of the three-dimensional structures of ribosomal particles in functionally relevant conformations. For this aim, we developed two approaches: (*a*) We crystallized and maintained the crystals under close-to-physiological conditions or (*b*) we activated the crystallized subunits and stabilized the so obtained conformation. Although neither of these approaches is simple or routine, we exploited them for the determination of high-resolution, functionally relevant structures of the small and large ribosomal subunits. These structures provide unique tools for the understanding of key questions concerning ribosomal function, mobility, dynamics, and integrity.

FLEXIBILITY, FUNCTIONAL ACTIVITY, AND DISORDER

Among the many crystal types that were obtained by us, the first to diffract to high resolution was that of the large ribosomal subunits from *H. marismortui* (66), the bacterium that lives in the Dead Sea, the lake with the highest salinity in the world. This bacterium withstands the high salinity as well as the elevated temperatures and has developed a sophisticated system to accumulate enormous amounts (3M) of KCl, although the medium contains only mM amounts of it (Table 1) (24). The reasons for the potassium intake are most probably not related to the ribosome function. However, the ribosomes of this bacterium adapted to the bacterial in situ environment, and their functional activity is directly linked to the concentration of potassium ions in the reaction mixture (Figure 1).

Initially, we grew the crystals of the 50S subunits from this bacterium (H50S) under conditions mimicking the interior of the bacteria at their log period. In these experiments, crystals were grown and kept in solutions containing all salts required to maintain a high functional activity of these halophilic ribosomes, including 3 M potassium chloride. Under these conditions, nucleation occurred rapidly and yielded small disordered crystals. Consequently, we developed a procedure for crystallization at the lowest potassium concentration required for maintaining the integrity of the subunits. Once the crystals grew, we transferred them to solutions containing ~3 M KCl, allowing the crystallized particles to rearrange into

TABLE 1 The concentration of ions within the cells of *Haloacula marismortui* [based on (24)]

	Early log	**Late log**	**Stationary**
K in cells:	3.7–5.0 M	3.7–4.0 M	3.7–4.0 M
Na in cells:	1.2–3.0 M	1.6–2.1 M	0.5–0.7 M

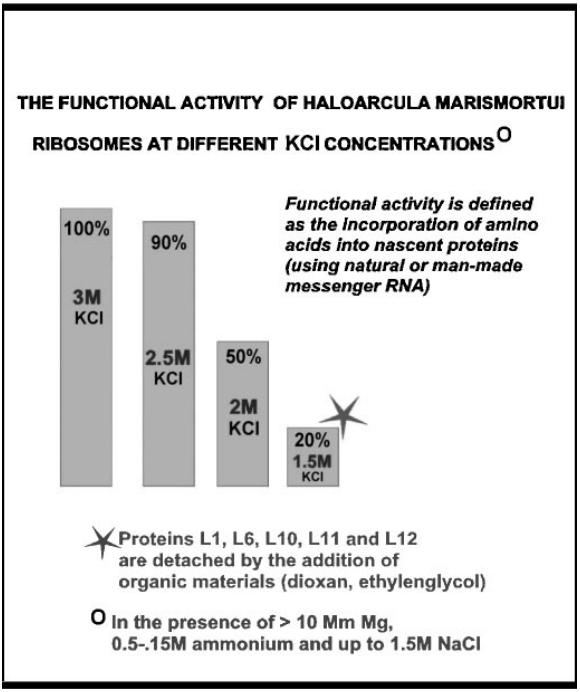

Figure 1 The functional activity of the ribosomes from *H. marismortui* at different potassium concentrations. Activity was checked by the synthesis of polypeptides and by the incorporation of 50S into 70S. In both cases, the ribosomal particles underwent heat activation at 55° for 40 min, and homo- or heteronucleotides served as mRNA chains.

their active conformation and regain their full functional activity. These crystals exhibited functional activity and diffracted well to high resolution (66, 73), but the high potassium concentration within them caused severe problems in the course of structure determination (29, 73). The combination of severe nonisomorphism, apparent twinning, high radiation sensitivity, unstable cell constants, nonuniform mosaic spread, and uneven reflection shape hampered the collection of data usable for structure determination. As these problems became less tolerable at higher resolution, the structure determination under close-to-physiological conditions stalled at resolutions lower than 5 Å (3, 29, 68, 73).

Improved crystals were obtained by drastic reduction (to mM amounts) of the salt concentration in their stabilization solution and by the exchange of high concentration of KCl by relatively low concentration of NaCl. These far-from-physiological conditions yielded a structure at 2.4 Å resolution (4) and even allowed the binding of compounds believed to be substrate analogs, such as CCdA-phosphate-puromycin (47). However, while under the far-from-physiological conditions, these ribosomes are less active in synthesis of proteins (56).

Several regions, including RNA helices and more than four proteins, were not observed in the 2.4 Å map of H50S (4). These were considered to be disordered. Almost all these untraceable regions are known to be heavily involved in the process of protein biosynthesis. Two of the RNA helical elements form intersubunit bridges, "the A-site finger" (H38) and the bridge reaching the decoding center (H69), within the assembled ribosome and interact with the tRNA molecules. The central loop of protein L5 forms the only intersubunit bridge made solely of proteins (together with protein S13 from the small subunit). Two additional proteins (L12 and L10) are involved in the contacts with the translocational factors and in factor-dependent GTPase activity (14), and protein L11 is involved in elongation factor activities (16). Protein L1 is a translational repressor binding mRNA (46), and its absence has a negative effect on the rate of protein synthesis (59).

All four proteins not observed in the 2.4 Å map match the list of proteins that we detached selectively from halophilic ribosomes (20). Furthermore, the low salt conditions used for the stabilization of the crystals are similar to those developed by us for the detachment of the selected proteins, namely the lowering of the salt concentration while adding modest amounts of organic materials. Evidently, these proteins are loosely held by the core of the large subunit, and it may well be that their level of disorder within the crystals allows partial or full removal from the large subunit. These crystals contain unusually large and continuous solvent regions (73) and accommodate materials the size of average ribosomal proteins (A. Bashan & J. Harms, unpublished data). Interestingly, the two major features not seen in the 2.4 Å map of H50S form the lateral protuberances, called the L1 stalk (H76-H78 with their bound protein L1) and the L12 stalk (H43-H44 and their bound proteins L10 and L12), that create the prominent features of the typical shape of the large subunit (Figure 2). Electron microscopy (EM), using negative staining, dark field, or cryo-EM reconstruction, readily observed both of them. These protruding stalk elements were also detected in electron density maps obtained from the crystals of H50S grown and maintained under close to physiological conditions (2, 73) albeit at lower resolution.

ARE THE INTERSUBUNIT BRIDGES DISORDERED IN UNBOUND RIBOSOMAL SUBUNITS?

All structural elements assumed to be disordered in the 2.4 Å structure of H50S were clearly detected in the 5.5 Å maps of the assembled 70S ribosome. This stimulated the notion that structural elements that interact with the small subunit or with ribosomal substrates are disordered in the unbound large subunit and may be stabilized in the 70S ribosome by intersubunit interactions or by their contacts with the tRNA molecules (75).

A possible cause for the disorder of the functionally relevant features in the 2.4 Å structure of H50S may be linked to the fact that these ribosomal particles were measured under conditions far from the in vivo situation. Biochemical, functional, and electron-microscopical studies indicate that these features are inherently

flexible, but flexibility is not necessarily synonymous with disorder. In many cases, flexible structural elements assume several well-defined conformations, and the switch from one conformation to another is related to their functional states. Detecting large disordered features in the high-resolution structure of H50S may indicate that the ribosomal strategy to avoid subunit association and substrate binding under far-from-physiological conditions is to introduce disorder in the relevant features.

To shed light on this intriguing question, we searched for a robust nonhalophilic bacterium as a potential source for suitable ribosomes. In parallel, we continued our efforts to elucidate the structure of H50S under close-to-physiological conditions. We recently calculated an electron density map from data collected from H50S crystals grown and kept under conditions mimicking the physiological environment of *H. marismortui* (I. Agmon, unpublished data). The resolution (3.6 Å) of our map is somewhat lower than that obtained for the crystals kept under far-from-physiological conditions. Nevertheless, the map is interpretable and enabled a rather detailed comparison between the two structures. The conformations of almost all the proteins in our structure differ to some extent from those observed under far-from-physiological conditions. The larger differences were observed in the locations and the internal order of the termini extensions. Under close-to-physiological conditions, more tails and extensions reach functionally important locations, such as tRNA-binding sites and intersubunit bridges. Also, many of the RNA regions disordered in the 2.4 Å map of H50S (4), such as helices H1, H38, and the L11 arm, are ordered. Thus, it is conceivable that the disorder of the features in the 2.4 Å structure of H50S reflects the strategy that the large subunit developed in order to avoid nonproductive association with the small subunit or with factors and substrates under far from natural conditions.

The search for a suitable mesophilic ribosome was stimulated by several reasons in addition to the apparent disorder of the functional elements of the 2.4 Å structure of H50S. *H. marismortui* is an archaea bearing low compatibility with *Escherichia coli*, the species yielding most of our knowledge on ribosomes. Despite the suitability of the ribosomes from *H. marismortui* for high-resolution crystallography, they have not become a subject of many biochemical studies. Consequently, only a small part of the vast amount of data of ribosomal research accumulated over almost half a century can be related directly to its structure. In addition, the antibiotics from the macrolide family hardly bind to the halophilic ribosomes because a key adenine is a guanine in their 23S RNA. They are also rather resistant to most of the antibiotic agents (40), even under suitable conditions. Thus, it is not surprising that contrary to the wealth of crystallographic information already obtained about binding of factors and antibiotics to the small subunit (9, 11, 12, 49, 50), only complexes of H50S with materials believed to represent substrate analogs were suitable for high-resolution crystallographic studies (47). Furthermore, despite extensive studies exploiting these complexes, the mechanism of the peptidyl-transferase activity is still not understood (5). In contrast to the strict requirements for antibiotics binding, all nucleotides crucial for the catalytic activity in the proposed mechanism

(47) could be mutated with little or no effect on peptide bond formation in vitro (51) and in vivo (62).

As mentioned above, we identified a robust ribosome from a mesophilic bacterium, *Deinococcus radiodurans* [and determined the 3.0 Å resolution structure of its large subunit (6, 28)]. The ribosome of this source shows a high homology to those of *T. thermophilus* and *E. coli*, and the crystals of its large subunit were grown and maintained under conditions almost identical to the bacterial in situ environment. These crystals, as well as those grown from complexes of these subunits with antibiotics, diffract to higher than 3 Å resolution, are relatively stable in the X-ray beam, and yield crystallographic data of high quality. Thus, they provide an excellent system to investigate antibiotic binding (54), shed light on the mechanism of peptide bond formation, and provide more insight into functional flexibility.

The structure of the large ribosomal subunit from *D. radiodurans*, *D50S*, as determined by us at 3 Å resolution, is significantly more ordered than that of H50S. Thus, most of the features that are disordered in H50S are well resolved in D50S (6, 28). Among the well-ordered features are the intersubunit bridges to the upper part of the small subunit (formed by helix H38) and to the decoding site (formed by H69), as well as the middle loop of protein L5, which forms the only intersubunit brige formed solely by ribosomal proteins "only protein" bridge. Also well ordered are the L1 arm (helices H76–H78) and the GTPase center (helices H42–H44 and protein L11). All display orientations that differ from those seen in the 5.5 Å structure of the 70S ribosome complex (75), which manifests their inherent flexibility.

Figure 3 demonstrates a feasible sequence of events leading to the creation of the intersubunit bridge, spanning from the large subunit to the decoding center on the small one. Helix H69, which is responsible for this bridge, lies in the unbound 50S subunit on the interface surface and interacts intensively with helix H70. Once the initiation complex, which includes the small subunit and tRNA at the P-site (see below for more detail), approaches the large subunit, the tRNA pushes helix H69 toward the decoding center, and the intersubunit bridge is formed.

The inherent flexibility of the ribosomal features is exploited also for controlling events in translocation. The comparison between the structure of the unbound 50S and the 70S ribosome indicates how the L1 arm facilitates the exit of the tRNA molecules. In the complex of T70S with three tRNA molecules, the L1 stalk interacts with the elbow of E-tRNA, and the exit path for the E-tRNA is blocked by proteins L1 from the large subunit and S7 from the small one (75). In the unbound mesophilic 50S, the L1 arm is tilted ~30 degrees away from its position in the T70S ribosome (Figure 4), and it does not block the presumed exit path of the E-site tRNA. Hence, the mobility of the L1 arm is utilized for facilitating the release of E-site tRNA. Superposition of the structure of the mesophilic unbound 50S on the T70S ribosome allowed the definition of a pivot point for a possible rotation of the L1 arm.

Our structure analysis showed that a similar strategy is taken when protein tails are involved in functional aspects. Almost all ribosomal proteins are built of

globular domains with extended tails or loops. Most of the globular domains are located on the solvent side of the particle, with their tails buried in the interior, and stabilize the RNA fold. However, the tails of a few proteins are pointing into the solution and are less engaged in RNA contacts. Some of these may make contributions to the efficient binding of nonribosomal factors participating in the process of protein biosynthesis by using their long tails as tentacles that enhance the correct positioning of the factors [as seen below and in (6, 25, 50)]. It is conceivable that the flexibility of these tails is also used for the reverse path. Once the binding is no longer required, the protein tails can stretch out, or become disordered, and release the compounds.

In general, the protein tails in the ribosomes that were kept close to their physiological environment seem to be more involved in protective interactions and reach closer to the functionally relevant sites than those maintained under nonphysiological conditions. Figure 5 shows examples for both tasks. The tail of protein L2 in the large subunit that was kept under physiological conditions (D50S) encloses and embraces an important RNA feature (H66), whereas the tail of the counterpart in the less physiologically relevant H50S particles folds away from the sensitive area. The second example is protein L27, which is located on the interface side of D50S at the base of the central protuberance (CP) in proximity to the peptidyl-transferase center, consistent with results of immune electron microscopy, protein-protein cross-linking, affinity labeling, chemical probing (57, 70), and footprinting (A. Mankin, personal communication). This protein has been implicated as a constituent of the peptidyl-transferase center of *E. coli* 50S by a variety of experimental observations. These include a deletion mutant that grows much slower than the wild type and shows deficiencies in the peptidyl-transferase activity and impaired enzymatic binding of Phe-tRNA Phe to the A-site. Although we did not resolve termini of four amino acids, in our structure it reaches the proximity of the P- and the A-sites, consistent with the proposal that it contributes to peptide bond formation by facilitating the proper placement of the acceptor end of the A-site tRNA (70). In contrast, the protein placed at the location of L27 in the 2.4 Å structure of H50S (called H21e) folds backward, toward the interior of the subunit, consistent with the hypothesis that the tails of the ribosomal proteins that bind factors and substrates fold away from the action sites when the conditions are not suitable for productive protein biosynthesis.

CONFORMATIONAL MOBILITY: THE KEY FOR SUBUNIT ASSOCIATION, DISSOCIATION, AND THE INITIATION OF PROTEIN BIOSYNTHESIS

The small ribosomal subunit is less stable than the large one. We found that by exposing 70S ribosomes to a potent proteolytic mixture, the 50S subunits remained intact, whereas the 30S subunits were completely digested (18). Similarly, large differences in the integrity of the two subunits were observed when attempting

crystallization of entire ribosomes assembled from purified subunits. Crystals obtained from these preparations consisted only of 50S subunits (7), and the supernatant of the crystallization drop did not contain intact small subunits but did show 30S proteins and a fragmented 16S RNA chain. Consequently, among the many ribosome sources that were tested, only the 30S from *T. thermophilus* (T30S) crystallized is suitable for crystallographic studies. Almost a decade was needed to minimize the severe nonisomorphism of this form, and all the procedures developed for increasing the homogeneity of these crystals are based on post-crystallization treatments. Our approach, described below and in (50, 53, 63), is to induce a specific conformation. Other approaches include treatment of the crystal by Co-hexamine (15, 69), a material known to bind specifically to RNA chains and increase their rigidity (13), or by spectinomycin (12), an antibiotic agent that locks the "head" (Figure 6) of the small subunit in a particular conformation (43).

The first task of the small subunit is to form the initiation complex; therefore, we assumed that the commonly used heat-activation procedure, developed over 30 years ago (76), induces the conformation required for this task. For obtaining small subunits at that particular conformation, we exposed our T30S crystals to elevated temperatures, according to the routine heat-activation procedure. Once activation was achieved, the conformation of the particles was stabilized (at ambient temperature) by incubation with minute amounts of a heteropolytungstate cluster, W18 (53, 63). The same procedure was employed for complexes of T30S with compounds that facilitate or inhibit protein biosynthesis, mRNA analogs, initiation factors, and antibiotics. Soaking in solutions containing the nonribosomal compounds in their normal binding buffer was performed at elevated temperatures. Once the functional complex was formed, the crystals were treated with the W18 cluster.

The initiation of protein biosynthesis has an important role in governing the accurate setting of the reading frame, as it facilitates the identification of the start codon of the mRNA. In prokaryotes, the initiation complex contains the small subunit, mRNA, three initiation factors (IF1, IF2-GTP, and IF3), and initiator tRNA. IF3 plays multiple roles in the formation of this complex. It influences the binding of the other ligands and acts as a fidelity factor by destabilizing noncanonical codon-anticodon interactions. It also selects the start-mRNA codon (37, 60) and the correct initiator tRNA to be positioned at the P-site (in prokaryotes, the fMET-tRNA). It stabilizes the binding of the fMet-tRNA/IF2 complex to 30S and discriminates against leaderless mRNA chains (42, 61). IF3 also acts as an anti-association factor because it binds with a high affinity to the 30S subunit and shifts the dissociation equilibrium of the 70S ribosome toward free subunits, thus maintaining a pool of 30S (26).

IF3 is a small basic protein of about 20 kD. It consists of C and N terminus domains (IF3C and IF3N) connected by a rather long lysine-rich linker region. The structure of the entire protein has not been determined, but NMR (22, 23) and X-ray structures of the N- and C-terminal domains have been reported (8, 36). The interdomain linker appears as a rigid alpha-helix only in the crystals containing it

and IF3N. However, the NMR studies showed that even under physiological conditions, the linker is partially unfolded and displays flexibility (17, 33, 34, 36, 45). Subsequently, the interdomain distances vary between 25 and 65 Å.

Crystals of the complex of T30S with IF3C were produced by heat activation and W18 stabilization. The conformation of the small subunits in this crystal is almost identical to that obtained by heat activation of the isolated particles (50). This indicates that activated and stabilized T30S has the conformation of the small subunit during the initiation phase of protein biosynthesis. It also explains why no major conformational changes were observed between the tungstenated and IF3C-bound 30S subunits, contrary to the conformational changes observed while binding IF3 to isolated 30S (21, 41). We therefore conclude that the conformation of the tungsten-bound 30S ribosomal subunit mimics that of the small subunit at the initiation stage and that the W18 cluster imitates the C-terminal domain of IF3 (Figures 6 and 7). Indeed, in competition experiments, crystals treated with W18 prior to soaking in solutions containing IF3C failed to bind IF3C.

Striking differences in the conformations of the proteins that bind IF3 (S18, S11, and S7) and of those interacting with them, such as protein S2, were detected by comparing the structure of isolated T30S (69) and that bound to IF3C (50). These proteins have tails and extended loops pointing toward the solution, in contrast to the majority of tails of ribosomal proteins that are buried within RNA features. An interesting example is protein S18. Its long terminus tails are more ordered in the tungstenated or IF3C-bound T30S than in the Co-hexamine-treated small subunits. These tails appear to act as tentacles that enhance the binding of IF3C, consistent with the firm binding of this domain to the ribosome (55, 67). They are also capable of binding the IF3C mimic, namely the W18 cluster (Figure 7).

The initiator mRNA in prokaryotes includes, along with the start codon, an upstream purine-rich sequence (SD, Shine-Dalgarno). This pairs with a complementary region in the 16S RNA (anti-SD) at its 3′ end, thus anchoring the mRNA chains. In the high-resolution structures of the 30S subunit, the anti-SD region is located on the solvent side of the platform, the region that also contains a large part of the E- site. Using crystals of T30S in complex with IF3C, IF3C binds to the 30S particle at the upper end of the platform on the solvent side (Figure 6), close to the anti-SD region of the 16S rRNA (50). This location reconfirms the results of NMR and mutagenesis of the IF3 molecule (55) and is compatible with the effect of the double mutations 1503, 1531 (19). It is also consistent with almost all the cross-links, footprints, and protection patterns reported for the *E. coli* system (38, 52).

CONFORMATIONAL MOBILITY GOVERNS SUBUNIT ASSOCIATION AND DISSOCIATION

It has been suggested that the C-terminal domain of IF3 (IF3C) performs many of the tasks assigned to the entire IF3 molecule: preventing the association of the 30S with the 50S subunit and contributing to the dissociation of the entire ribosome (30).

IF3C also influences the formation of the initiation complex. The ability of IF3 to discriminate noncanonical initiation codons, or to verify codon-anticodon complementarity, has been attributed mainly to IF3N (10).

The location of IF3C we observed suggests that the binding of IF3C to the 30S subunit influences the mobility of the platform near the anchoring site of the SD sequence. The binding at this site could affect the conformational mobility of the platform, essential for the association of the two ribosomal subunits to form a productive ribosome, consistent with biochemical observations indicating that IF3C prevents subunit association or promotes dissociation by influencing the conformational dynamics of the subunit. The spatial proximity of the IF3C-binding site to the anti-SD region suggests a connection between them. These interactions could suppress the change in the conformational dynamics induced by IF3, thus allowing subunit association. The connection between the double mutation of G1530/A1531 to A1530/G1531 and the reduced IF3 binding to the 30S subunit, together with the enhanced affinity of IF3 to the 70S ribosomes, supports this hypothesis.

The placement of IF3C on the solvent side of the upper platform sheds light on the initial step of protein biosynthesis, which involves the detachment of the SD sequence. This region is also involved in the displacement of the platform that accompanies the translocation (21), as part of the combined head-platform-shoulder conformational changes. The binding of IF3C and the hybridization of the anti-SD sequence limit the mobility of this region. Upon the detachment of the SD anchor, required at the beginning of the translocation process, the platform may regain its conformational mobility. The bound IF3N leaves a limited, albeit sufficient, space for P-site tRNA, and only small conformational changes are required for simultaneous binding of IF3N, mRNA, and the P-site tRNA. Thus, the influence of IF3N on initiator tRNA binding is based on space-exclusion principles rather than on specific codon-anticodon complementarity rules, as suggested earlier (41).

Only indirect contacts exist between IF3N and IF3C, via the curved connection formed by the interdomain linker that wraps around the platform toward the neck. Various mutations, insertions, and deletions that cause significant modifications in the length of the linker do not have major effects on the efficiency of IF3, which indicates that the linker maintains its flexibility while IF3 is bound to the 30S subunit. Consequently, it can act as a transmitting strap between the two domains and can indirectly affect the conformation of the P-site and induce its specificity (17). Similarly, the structural changes in IF3 could trigger conformational changes within the 30S subunit that are required for initiating the biosynthetic process and may also lead to a suppression of secondary-structure elements in the mRNA. Thus, our placement is consistent with the proposal that the linker maintains its flexibility when IF3 is bound to the 30S subunit and that the flexibility and the ability of the linker region to alter its fold are related to the function of IF3.

Support for the placement of IF3, and for the mechanism inferred from it, is provided by the analysis of the mode of action and the location of edeine (Figure 8), a

universal antibiotic agent that interferes with the initiation process (1, 48). Edeine is a peptide-like antibiotic agent, produced by a strain of *Bacillus brevis*. It contains a spermidine-type moiety at its C-terminal end and a beta-tyrosine residue at its N-terminal end (35). Using crystals of the complex of edeine with T30S, we found that edeine binds in the solvent side of the platform. It also induces the formation of a new base pair between two helices of the platform. In its position, edeine would not alter IF3C binding but might well affect the binding of the linker and hence the binding of IF3N. At the same time, it could affect the 30S mobility, the interaction of the 3′ end with IF3C, and the interaction of the 30S and 50S subunits because it connects the penultimate helix (H44) with the major constituents of the platform. By physically linking these components, edeine can lock the small subunit (Figure 8) and hinder the conformational changes that accompany the translation process (21, 65). Independent studies show that pactamycin, an antibiotic agent that shares a protection pattern with edeine, bridges the same helices linked by the edeine-induced base pair (9). Pactamycin is also known to interfere with the initiation process, and its mode of interaction suggests that it may interfere with the pairing of the SD sequence or prevent it.

The universal effect of edeine on initiation implies that the main structural elements important for the initiation process are conserved in all kingdoms (48). Our results show that the rRNA bases that bind edeine are conserved in chloroplasts, mitochondria, and the three phylogenetic domains. Electron microscopy studies on rat liver 40S in complex with the eukaryotic IF3 located it in a region comparable to our findings (58). In this location, IF3 and its eukaryotic counterpart seem to perform their anti-association activity by affecting the conformational mobility of the small ribosomal subunit: in particular, suppressing the conformational mobility of the platform, essential for association of the two ribosomal subunits. Some aspects of the initiation process of protein biosynthesis were different in eukaryotic and prokaryotic systems (31). Nevertheless, neither indicate different locations of IF3. The consistency between our results and the location of the eukaryotic IF may indicate that the main concepts underlying the initiation process and governing the anti-association properties of the initiation complex have been evolutionarily conserved.

CONCLUDING REMARKS

Ribosomal crystallography, initiated two decades ago, recently yielded an impressive amount of exciting structural information. This chapter relates to characteristics common to all available structures and describes our analyses of selected conformations of the two ribosomal subunits at various functional states. These studies identified the structural elements involved in the dynamics of protein biosynthesis and showed that exploiting inherent flexibility for controlling the functional needs of the ribosome is the general strategy taken by the ribosome. By comparing the structures obtained from conditions far and close to physiological ones, we learned that the ribosome exploits this built-in flexibility as a natural tool for preventing nonproductive binding of factors or intersubunit interactions. This is

achieved either by folding the tails of the binding proteins away from the binding sites or by inducing significant disorder, as seen in the 2.4 Å structure of the large ribosomal subunit from *H. marismortui* because it represents a conformation that differs from that of the native particle. Still to be revealed is the high-resolution structure of the entire ribosome and the mechanism of peptide bond formation. The need for additional structures required to answer specific questions is evident. However long-lasting the search has been already, it is not over yet, and the reality of understanding the mechanisms of translation by the ribosome are enticing prospects for the future.

ACKNOWLEDGMENTS

These studies were performed at the Structural Biology Department of the Weizmann Institute, the Max-Planck Research Unit for Ribosomal Structure, and in the Max-Planck Institute for Molecular Genetics in Berlin. Thanks are given J. M. Lehn for indispensable advice; M. Pope for the tungsten clusters; R. Wimmer for recommending the ribosomal source; and M. Wilchek, W. Traub, L. Shimon, and A. Mankin for critical discussions. These studies could not be performed without the cooperation and assistance of the staff of the synchrotron radiation facilities at EMBL and MPG at DESY; ID14/2&4 at EMBL/ESRF and ID19/APS/ANL. The Max-Planck Society, the U.S. National Institutes of Health (GM34360), the German Ministry for Science and Technology (Bundesministerium für Bildung, Wissenschaft, Forschung und Technologie Grant 05-641EA) and the Kimmelman Center for Macromolecular Assembly at the Weizmann Institute provided support. A. Yonath holds the Martin S. Kimmel Professorial Chair.

LITERATURE CITED

1. Altamura S, Sanz JL, Amils R, Cammarano P, Londei P. 1988. The antibiotic sensitivity spectra of ribosomes from the thermoproteales phylogenetic depth and distribution of antibiotic binding sites. *Syst. Appl. Microbiol.* 10:218–25
2. Ban N, Freeborn B, Nissen P, Penczek P, Grassucci RA, et al. 1998. A 9 Å resolution X-ray crystallographic map of the large ribosomal subunit. *Cell* 93:1105–15
3. Ban N, Nissen P, Hansen J, Capel M, Moore P, Steitz TA. 1999. Placement of protein and RNA structures into a 5 Å resolution map of the 50S ribosomal subunit. *Nature* 400:841–47
4. Ban N, Nissen P, Hansen J, Moore PB, Steitz TA. 2000. The complete atomic structure of the large ribosomal subunit at 2.4 Å resolution. *Science* 289:905–20
5. Barta A, Dorner S, Polacek N. 2001. Mechanism of ribosomal peptide bond formation. *Science* 291:203–4
6. Bashan A, Agmon I, Zarivach R, Schlünzen F, Harms J, et al. 2001. *High Resolution Structures of Ribosomal Subunits: Initiation, Inhibition and Conformational Variability*. New York: Cold Spring Harbor. In press
7. Berkovitch-Yellin Z, Bennett WS, Yonath A. 1992. Aspects in structural studies on ribosomes. *CRC Rev. Biochem. Mol. Biol.* 27:403–44

8. Biou V, Shu F, Ramakrishnan V. 1995. X-ray crystallography shows that translational initiation factor IF3 consists of two compact alpha/beta domains linked by an alpha-helix. *EMBO J.* 14:4056–64
9. Brodersen DE, Clemons WM Jr, Carter AP, Morgan-Warren RJ, Wimberly BT, et al. 2000. The structural basis for the action of the antibiotics tetracycline, pactamycin and hygromycin B on the 30S ribosomal subunit. *Cell* 103:1143–54
10. Bruhns J, Gualerzi CO. 1980. Structure-function relationship in *E. coli* initiation factors: role of tyrosine residues in ribosomal binding and functional activity of IF-3. *Biochemistry* 19:1670–76
11. Carter AP, Clemons WM Jr, Brodersen DE, Morgan-Warren RJ, Hartsch T, et al. 2001. Crystal structure of an initiation factor bound to the 30S ribosomal subunit. *Science* 291:498–501
12. Carter AP, Clemons WM Jr, Brodersen DE, Morgan-Warren RJ, Wimberly BT, et al. 2000. Functional insights from the structure of the 30S ribosomal subunit and its interactions with antibiotics. *Nature* 407:340–48
13. Cate JH, Doudna JA. 1996. Metal-binding site in the major groove of a large ribozyme domain. *Structure* 4:1221–29
14. Chandra Sanyal S, Liljas A. 2000. The end of the beginning: structural studies of ribosomal proteins. *Curr. Opin. Struct. Biol.* 10:633–36
15. Clemons WM Jr, Brodersen DE, McCutcheon JP, May JLC, Carter AP, et al. 2001. Crystal structure of the 30S ribosomal subunit from *Thermus thermophilus*: purification, crystallization and structure determination. *J. Mol. Biol.* 310:827–43
16. Cundliffe E, Dixon P, Stark M, Stoffler G, Ehrlich R, et al. 1979. Ribosomes in thiostrepton-resistant mutants of *Bacillus megaterium* lacking a single 50S subunit protein. *J. Mol. Biol.* 132:235–52
17. de Cock E, Springer M, Dardel F. 1999. The inter domain linker of *E. coli* initiation factor IF3: a possible trigger of translation initiation specificity. *Mol. Microbiol.* 32:193–202
18. Evers U, Franceschi F, Boeddeker N, Yonath A. 1994. Crystallography of halophilic ribosome: the isolation of an internal ribonucleoprotein complex. *Biophys. Chem.* 50:3–16
19. Firpo MA, Connelly MB, Goss DJ, Dahlberg AE. 1996. Mutations at two invariant nucleotides in the 3′-minor domain of *E. coli* 16S rRNA affecting translational initiation and initiation factor 3 function. *J. Biol. Chem.* 271:4693–98
20. Franceschi F, Sagi I, Boeddeker N, Evers U, Arndt E, et al. 1994. Crystallography, biochemical and genetics studies on halophilic ribosomes. *Syst. Appl. Microbiol.* 16:697–705
21. Gabashvili I, Grawal RK, Grassucci R, Frank J. 1999. Structure and structural variations of the *E. coli* 30S ribosomal subunit as revealed by three-dimensional cryo-electron microscopy. *J. Mol. Biol.* 286: 1285–91
22. Garcia C, Fortier P, Blanquet S, Lallemand J-Y, Dardel F. 1995. ^{1}H and ^{15}N resonance assignment and structure of the N-terminal domain of *Escherichia coli* initiation factor 3. *Eur. J. Biochem.* 228:395–402
23. Garcia C, Fortier P, Blanquet S, Lallemand J-Y, Dardel F. 1995. Solution structure of the ribosome-binding domain of *E. coli* translation initiation factor IF3. Homology with U1A protein of the eukaryotic spliceosome. *J. Mol. Biol.* 254:247–59
24. Ginzburg M, Sacks L, Ginzburg BZ. 1970. Ion metabolism in *Halobacterium*. *J. Gen. Physiol.* 55:178–207
25. Gluehmann M, Harms J, Zarivach R, Bashan A, Schlünzen F, Yonath A. 2001. Ribosomal crystallography: from poorly diffracting micro-crystals to high resolution structures. *Methods* In press
26. Grunberg-Manago M, Dessen P, Pantaloni D, Godefroy-Colburn T, Wolfe AD, et al. 1975. Light-scattering studies showing the effect of initiation factors on the reversible

dissociation of *E. coli* ribosomes. *J. Mol. Biol.* 94:461–78
27. Hansen HAS, Volkmann N, Piefke J, Glotz C, Weinstein S, Makowski I, et al. 1990. Crystals of complexes mimicking protein biosynthesis are suitable for crystallographic studies. *Biochim. Biophys. Acta* 1050:1–7
28. Harms J, Schlünzen F, Zarivach R, Bashan A, Gat S, et al. 2001. High-resolution structure of the large ribosomal subunit from a mesophilic eubacterium. *Cell* 107:1–20
29. Harms J, Tocilj A, Levin I, Agmon I, Stark H, et al. 1999. Elucidating the medium-resolution structure of ribosomal particles: an interplay between electron cryomicroscopy and X-ray crystallography. *Struct. Fold Des.* 7:931–41
30. Hershey JW. 1987. Protein synthesis. In *ASM Molecular Biology*, ed. F Neidhardt, J Ingraham, K Low, B Magasanik, M Schaechter, H Umbarger, pp. 613–47. Washington, DC: ASM
31. Hershey JW, Asano K, Naranda T, Vornlocher HP, Hanachi P, Merrick WC. 1996. Conservation and diversity in the structure of translation initiation factor EIF3 from humans and yeast. *Biochimie* 78:903–7
32. Hope H, Frolow F, von Boehlen K, Makowski I, Kratky C, et al. 1989. Cryo crystallography of ribosomal particles. *Acta Crystallogr. B* 345:190
33. Hua YX, Raleigh DP. 1998. Conformational analysis of the inter domain linker of the central homology region of chloroplast initiation factor IF3 supports a structural model of two compact domains connected by a flexible tether. *FEBS Lett.* 433:153–56
34. Hua YX, Raleigh DP. 1998. On the global architecture of initiation factor IF3: a comparative study of the linker regions from the *E. coli* protein and the *Bacillus stearothermophilus* protein. *J. Mol. Biol.* 278:871–78
35. Kurylo-Borowska Z. 1975. Biosynthesis of edeine. II. Localization of edeine synthetase within *Bacillus brevis* Vm4. *Biochim. Biophys. Acta* 399:31–41
36. Kycia JH, Biou V, Shu F, Gerchman SE, Graziano V, et al. 1995. Prokaryotic translation initiation factor IF3 is an elongated protein consisting of two crystallizable domains. *Biochemistry* 34:6183–87
37. La Teana A, Gualerzi CO, Brimacombe R. 1995. From stand-by to decoding site. Adjustment of the mRNA on the 30S ribosomal subunit under the influence of the initiation factors. *RNA* 1:772–82
38. Mackeen LA, Kahan L, Wahba AJ, Schwartz I. 1980. Photochemical cross-linking of initiation factor-III to *Escherichia coli* 30S ribosomal-subunits. *J. Biol. Chem.* 255:526–31
39. Makowski I, Frolow F, Shoham M, Wittmann HG, Yonath A. 1987. Single crystals of large ribosomal particles from *H. marismortui* diffract to 6 Å. *J. Mol. Biol.* 193: 819–22
40. Mankin AS, Garrett RA. 1991. Chloramphenicol resistance mutations in the single 23S rRNA gene of archaeon *Halobacterium halobium*. *J. Bacteriol.* 173:3559–63
41. McCutcheon JP, Agrawal RK, Philips SM, Grassucci RA, Gerchman SE, et al. 1999. Location of translational initiation factor IF3 on the small ribosomal subunit. *Proc. Natl. Acad. Sci. USA* 96:4301–6
42. Meinnel T, Sacerdot C, Graffe M, Blanquet S, Springer M. 1999. Discrimination by *E. coli* initiation factor IF3 against initiation on non-canonical codons relies on complementarity rules. *J. Mol. Biol.* 290:825–37
43. Moazed D, Noller HF. 1987. Interaction of antibiotics with functional sites in 16S rRNA. *Nature* 327:389–94
44. Moazed D, Samaha RR, Gualerzi C, Noller HF. 1995. Specific protection of 16S rRNA by translational initiation factors. *J. Mol. Biol.* 248:207–10
45. Moreau M, Coch E, Fortier PL, Garcia C, Albaret C, et al. 1997. Heteronuclear NMR studies of *E. coli* translation initiation factor IF3. Evidence that the inter-domain region is disordered in solution. *J. Mol. Biol.* 266:15–22

46. Nikonov S, Nevskaya N, Eliseikina I, Fomenkova N, Nikulin A, et al. 1996. Crystal structure of the RNA binding ribosomal protein L1 from *Thermus thermophilus*. *EMBO J.* 15:1350–59
47. Nissen P, Hansen J, Ban N, Moore PB, Steitz TA. 2000. The structural basis of ribosome activity in peptide bond synthesis. *Science* 289:920–30
48. Odon OW, Kramer G, Henderson AB, Pinphanichakarn P, Hardesty B. 1978. GTP hydrolysis during methionyl-tRNAf binding to 40S ribosomal subunits and the site of edeine inhibition. *J. Biol. Chem.* 253:1807–16
49. Ogle JM, Brodersen DE, Clemons WM Jr, Tarry MJ, et al. 2000. Recognition of cognate transfer RNA by the 30S ribosomal subunit. *Science* 292:897–902
50. Pioletti M, Schlünzen F, Harms J, Zarivach R, Gluhmann M, et al. 2001. Crystal structures of complexes of the small ribosomal subunit with tetracycline, edeine and IF3. *EMBO J.* 20:1829–39
51. Polacek N, Gaynor M, Yassin A, Mankin AS. 2001. Ribosomal peptidyl transferase can withstand mutations at the putative catalytic nucleotide. *Nature* 411:498–501
52. Sacerdot C, de Cock E, Engst K, Graffe M, Dardel F, Springer M. 1999. Mutations that alter initiation codon discrimination by *Escherichia coli* initiation factor IF3. *J. Mol. Biol.* 288:803–10
53. Schlünzen F, Tocilj A, Zarivach R, Harms J, Glühmann M, et al. 2000. Structure of functionally activated small ribosomal subunit at 3.3 angstrom resolution. *Cell* 102:615–23
54. Schlünzen F, Zarivach R, Harms J, Bashan A, Tocilj A, et al. 2001. Structural basis for the interaction of five antibiotics with the peptidyl transferase center in eubacteria. *Nature* 413:814–21
55. Sette M, Spurio R, Van Tilborg P, Gualerzi CO, Boelens R. 1999. Identification of the ribosome binding sites of translation initiation factor IF3 by multidimensional heteronuclear NMR spectroscopy. *RNA* 5:82–92
56. Shevack A, Gewitz HS, Hennemann B, Yonath A, Wittmann HG. 1985. Characterization and crystallization of ribosomal practical from *H. marismortui*. *FEBS Lett.* 184:68–73
57. Sonenberg N, Wilchek M, Zamir A. 1973. Mapping of *E. coli* ribosomal components involved in peptidyl transferase activity. *Proc. Natl. Acad. Sci. USA* 70:1423–26
58. Srivastava S, Verschoor A, Frank J. 1992. Eukaryotic initiation factor-III does not prevent association through physical blockage of the ribosomal-subunit interface. *J. Mol. Biol.* 226:301–4
59. Subramanian AR, Dabbs ER. 1980. Functional studies on ribosomes lacking protein L1 from mutant *Escherichia coli*. *Eur. J. Biochem.* 112:425–30
60. Sussman JK, Simons EL, Simons RW. 1996. *E. coli* translation initiation factor 3 discriminates the initiation codon in vivo. *Mol. Microbiol.* 21:347–60
61. Tedin K, Moll I, Grill S, Resch A, Graschopf A, et al. 1999. Translation initiation factor 3 antagonizes authentic start codon selection on leaderless mRNAs. *Mol. Microbiol.* 31:67–77
62. Thompson J, Kim DF, O'Connor M, Lieberman KR, Bayfield MA, et al. 2001. Analysis of mutations at residues A2451 and G2447 of 23S rRNA in the peptidyltransferase active site of the 50S ribosomal subunit. *Proc. Natl. Acad. Sci. USA* 98: 9002–7
63. Tocilj A, Schlünzen F, Janell D, Gluehmann M, Hansen HAS, et al. 1999. The small ribosomal subunit from *T. thermophilus* at 4.5 Å resolution: pattern fittings and the identification of a functional site. *Proc. Natl. Acad. Sci. USA* 96:14252–57
64. Trakhanov SD, Yusupov MM, Agalarov SC, Garber MB, Ryazantsev SN, et al. 1987. Crystallization of 70S ribosomes and 30S ribosomal subunits from *Thermus thermophilus. FEBS Lett.* 220:319–22

65. VanLoock MS, Agrawal RK, Gabashvili I, Frank J, Harvey SC. 2000. Movement of the decoding region of the 16S ribosomal RNA accompanies tRNA translocation. *J. Mol. Biol.* 304:507–15
66. von Boehlen K, Makowski I, Hansen HA, Bartels H, Berkovitch-Yellin Z, et al. 1991. Characterization and preliminary attempts for derivatization of crystals of large ribosomal subunits from *Haloarcula marismortui* diffracting to 3 Å resolution. *J. Mol. Biol.* 222:11–15
67. Weiel J, Hershey JW. 1981. Fluorescence polarization studies of the interaction of *E. coli* protein synthesis initiation factor 3 with 30S ribosomal subunits. *Biochemistry* 20:5859–65
68. Weinstein S, Jahn W, Glotz C, Schlünzen F, Levin I, et al. 1999. Metal compounds as tools for the construction and the interpretation of medium-resolution maps of ribosomal particles. *J. Struct. Biol.* 127:141–51
69. Wimberly BT, Brodersen DE, Clemons WM Jr, Morgan-Warren RJ, Carter AP, et al. 2000. Structure of the 30S ribosomal subunit. *Nature* 407:327–39
70. Wower IK, Wower J, Zimmermann RA. 1998. Ribosomal protein L27 participates in both 50S subunit assembly and the peptidyl transferase reaction. *J. Biol. Chem.* 273:19847–52
71. Yonath A, Bartunik AD, Bartels K, Wittmann HG. 1984. Some X-ray diffraction patterns from single crystals of the large ribosomal subunit from *Bacillus stearothermophilus*. *J. Mol. Biol.* 177:201–6
72. Yonath A, Glotz C, Gewitz HS, Bartels KS, von Bohlen K, et al. 1988. Characterization of crystals of small ribosomal subunits. *J. Mol. Biol.* 203:831–34
73. Yonath A, Harms J, Hansen HAS, Bashan A, Schlünzen F, et al. 1998. Crystallographic studies on the ribosome, a large macromolecular assembly exhibiting severe non-isomorphism, extreme beam sensitivity and no internal symmetry. *Acta Crystallogr. A* 54:945–55
74. Yonath A, Mussig J, Tesche B, Lorenz S, Erdmann V, Wittmann HG. 1980. *Biochem. Int.* 1, 428:31–35
75. Yusupov MM, Yusupova GZ, Baucom A, Lieberman K, Earnest TN, et al. 2001. Crystal structure of the ribosome at 5.5 Å resolution. *Science* 292:883–96
76. Zamir A, Miskin R, Elson D. 1971. Inactivation and reactivation of ribosomal subunits: amino acyl transfer RNA binding activity of the 30S subunit from *E. coli. J. Mol. Biol.* 60:347–64

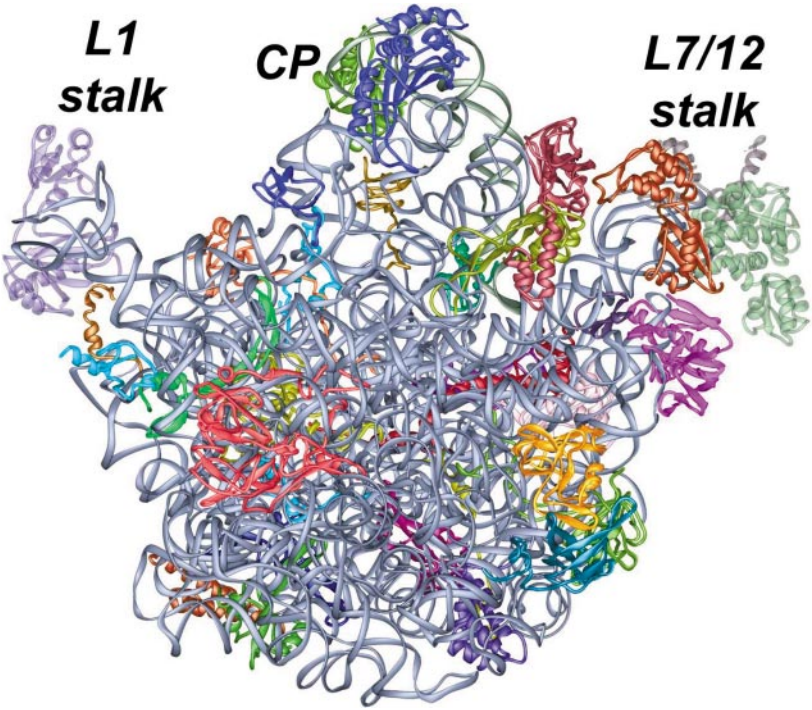

Figure 2 The current "crown view" of D50S. The RNA is shown as *gray-blue* ribbons and the proteins are in different colors. For orientation, the L1 arm is on the left, and the L7/12 arm is on the right.

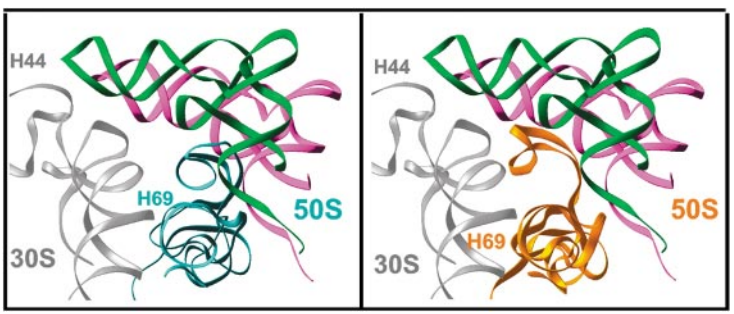

Figure 3 The intersubunit bridge formed by helix H69. In both parts, the small subunit is placed on the left side and the large subunit on the right. Helix H44 of the small subunit is shown in *gray*. The decoding center is on its upper side. Also shown are the docked tRNA molecules (P-site tRNA in *magenta* and A-site tRNA in *green*). Coordinates of the small subunit and the two tRNA sites were taken from (75). For clarity, the mRNA is not shown. The *left box* shows the shape of H69 in the large (50S) subunit, just before the approach of the initiation complex (the small subunit, P-site tRNA, and the initiator mRNA). In this position, H69 interacts with its neighbors in the 50S subunit. The approaching tRNA pushes H69 toward the small subunit until it reaches its bound conformation (in *gold*), as determined in the 70S complex (75).

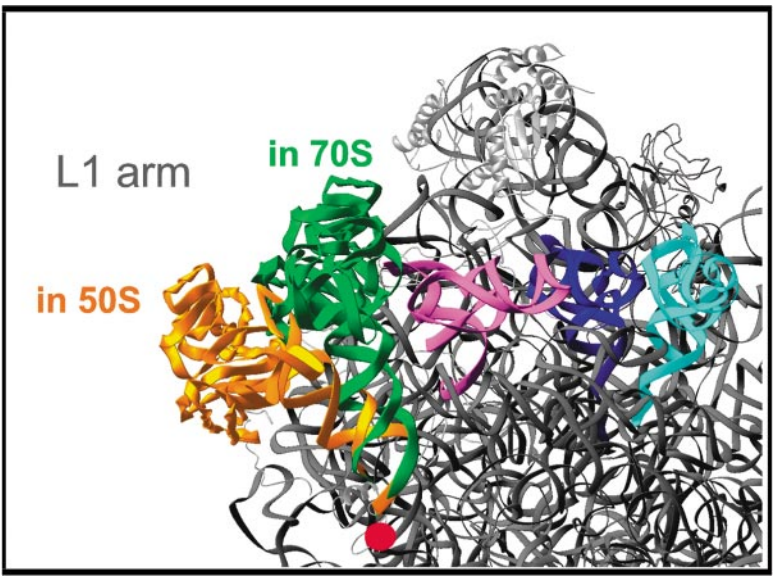

Figure 4 Part of the upper side of the view shown in Figure 2, with the L1 stalk on the left. The flexibility of the L1 arm may be exploited to form a gate for the exiting tRNA molecules. The *gold* feature represents its position in the unbound D50S subunit, and the *green* represents its position in the entire ribosome. *Red* indicates the pivot point. In the complex of the whole ribosome with three tRNA molecules (75), this arm assumes a conformation that may correspond to a "closed-gate," trapping the E-site tRNA (in *magenta*). The conformation seen in the unbound 50S subunit may represent the "open-gate" state.

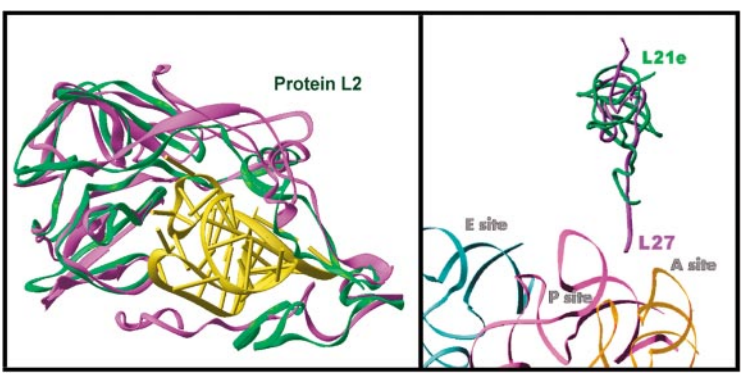

Figure 5 *Left*: Protein L2 (*purple*, in H50S; *green*, in D50S). Helix H66 is shown in *yellow*. Note the remarkable differences in the conformations of parts of the globular domains and of the C-terminal tails. In D50S the latter embraces and stabilizes the RNA helix H66. In H50S, in contrast, it folds backward on itself away from the helix. *Right*: The D50S protein L27 and its tail that extends toward the A- and P-site tRNAs. Protein L27 does not exist in the halophilic ribosome, and its position is occupied by a protein that shows no sequence similarity to L27 (called L21e and shown in *green*). The tail of L21e folds backward, away from the tRNA-binding sites.

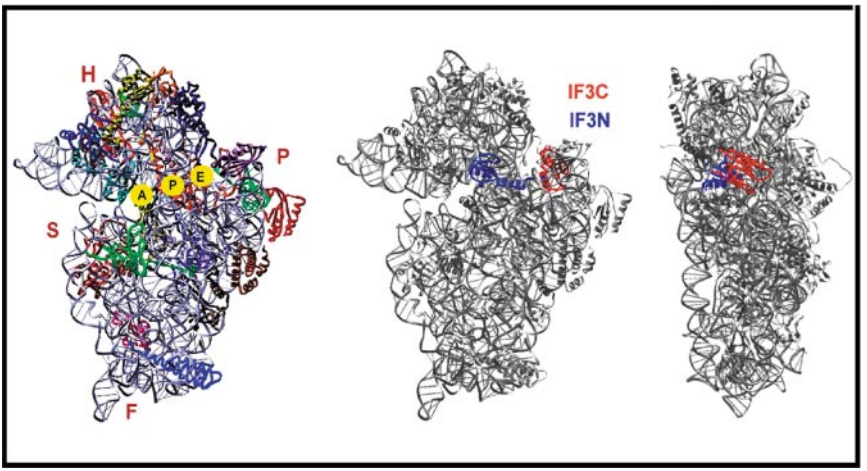

Figure 6 *Left*: The small subunit seen from the interface side (the side facing the large subunit in the 70S ribosome). The RNA is shown as simple ribbons, in *silver*. The proteins are in different colors. The major subdivisions are labeled: H, head; S, shoulder; P, platform; F, foot. The approximate locations of A-, P-, and E-tRNA-binding sites are marked. *Middle*: The same view of the small subunit as on the left, but the entire subunit is drawn in *gray*. The location of IF3 is marked in *red* (for the C-terminal domain, IF3C) and in *blue* (the N-terminal domain, IF3N, and the intersubunit linker). *Right*: Side view of the mall subunit, with its platform pointing toward the reader (obtained by 90° rotation about the long axis of the left and the middle views).

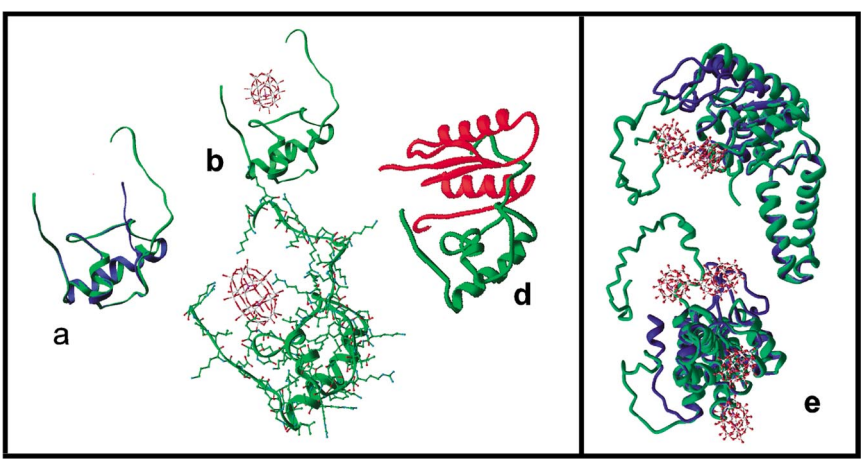

Figure 7 The conformations of proteins L18 (*left*) and L2 (*right*) as detected in the tungstenated (in *green*) and the nontungstenated (*dark blue*) forms of T30S. The W atoms are shown in *red*. (*a*) Superposition of the two structures of protein S18. (*b*, *c*) The general fold and the specific contacts formed between the terminal tails of protein S18 and the W18 cluster. (*d*) The binding of IF3C to the 30S subunit. Most of the contacts are formed by protein S18. Note the remarkable similarities in IF3C and W18 binding by the tails of S18. (*e*) Superposition of the two structures of protein S2.

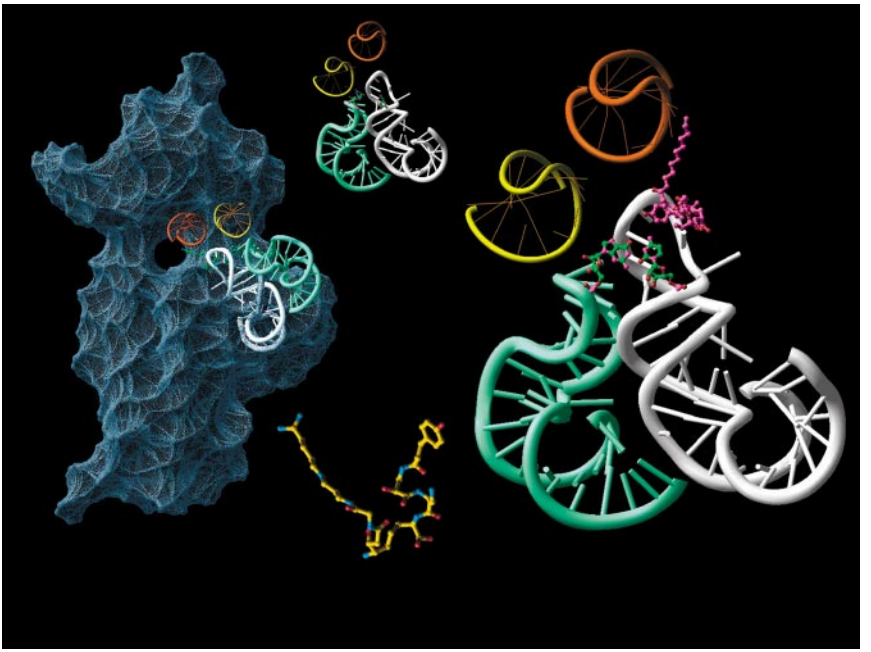

Figure 8 The binding of the universal antibiotic edeine to the small subunit. *Left*: An overall view (color code of the helical elements as described below). The small subunit is shown at about 75° rotation (around the vertical axis of the particle) compared to the view of the left side of Figure 6. The mRNA channel is clearly seen and the sites of P- (*orange*) and E- (*yellow*) are indicated. *Right*: Close-up of edeine-binding area. H23 is shown in *light green*, and H24 in *white*. Edeine is *pink*, and the newly formed base pair is *green*. The inhibitory action of this antibiotic—interfering with the initiation process by limiting the mobility of the platform—is evident. *Inserts*: *Top*: The edeine-binding region (as shown on the right) in its unbound state. *Bottom*: The chemical formula of edeine.